

Explosion Gravitation Field Algorithm with Dust Sampling for Unconstrained Optimization

Xuemei Hu¹, Lan Huang^{1,2}, Yan Wang^{1,*}, Wei Pang^{3,4*}

¹College of Computer Science and Technology, Jilin University. Changchun, 130012, China.

Key Laboratory of Symbol Computation and Knowledge Engineering of Ministry of Education, Jilin University. Changchun, 130012, China.

²Zhuhai Laboratory of Key Laboratory of Symbolic Computation and Knowledge Engineering of Ministry of Education, Department of Computer Science and Technology, Zhuhai College of Jilin University, Zhuhai, 519041, China.

³Department of Computing Science, University of Aberdeen, AB24 3UE, United Kingdom.

⁴Shaanxi Key Laboratory of Complex System Control and Intelligent Information Processing, Xi'an 710048, China

Corresponding authors: wy6868@jlu.edu.cn; pang.wei@abdn.ac.uk

Abstract

Gravitation Field Algorithm (GFA) is a novel optimization algorithm derived from the Solar Nebular Disk Model (SNDM) in astronomy and inspired by the formation process of planets. Although it has achieved good performance when solving many unconstrained optimization problems, which demonstrated its promising application potential in many real-world problems, GFA still has much room for improvement, especially when it comes to the accuracy and efficiency of the algorithm.

In this research, an improved GFA algorithm called Explosion Gravitation Field Algorithm (EGFA) is proposed for unconstrained optimization problems, with the introduction of two strategies: Dust Sampling (DS) and Explosion Operation. The task of DS is to locate the space that contains the optimal solution(s) by initializing the dust population randomly in the problem search space; while the Explosion Operator is to improve the accuracy of solutions and decrease the probability of the algorithm falling into local optima by generating the new population around the center dust to replace the original population.

A comparison of experimental results on six classical unconstrained benchmark problems with different dimensions demonstrates that the proposed EGFA outperforms the original GFA and several classical metaheuristic optimization algorithms, such as Genetic Algorithm (GA) and Particle Swarm

29 Optimization (PSO), in terms of accuracy and efficiency in lower dimensions. Additionally, the
30 comparison of results on three real datasets indicate that EGFA performs better than the original GFA
31 and k-means for solving clustering problems.

32 **Key words:**

33 Explosion gravitation field algorithm; Unconstrained optimization; Dust Sampling; Explosion operation

34 **1. Introduction**

35 Optimization problems exist in almost all fields of science and engineering, and they can be divided into
36 two categories in terms of if there exist constrained conditions upon these problems: constrained
37 optimization problems and unconstrained ones. Unconstrained optimization problems have been studied
38 extensively for a long time, but we are still facing challenges in acquiring desirable solutions for many
39 of these problems in terms of accuracy and efficiency. Traditional mathematical methods for solving
40 these unconstrained optimization problems, such as the steepest descent method [1], the Newton method
41 [2], the conjugate gradient method [3], and the quasi-Newton method [4], normally require or assume
42 that the optimization problems are continuous and differentiable and often some prior knowledge is
43 needed in advance. This makes it challenging for the above traditional algorithms to solve problems of
44 higher dimensions.

45 To address the above challenges, many novel computational intelligence (CI) algorithms have been
46 proposed over the past several decades, some of which have broken through the above rigorous
47 limitations effectively. The significant advantages enable CI algorithms to be widely adopted to solve
48 many unconstrained optimization problems. Over the past two decades, there have been many effective
49 computational intelligence algorithms proposed, which are inspired by natural phenomena. For instance,
50 Simulated Annealing (SA) algorithm proposed by Metropolis *et al.* in 1953 was inspired by annealing in
51 metallurgy. Genetic algorithm (GA) [5][6], originally proposed by Holland in 1975, emulates the natural
52 evolution selection process, and it is based on the Darwinian biological evolution theory. Ant colony
53 optimization (ACO) [7][8] proposed by Dorigo in 1992 is based on the heuristic process of ant's food
54 discovery and incorporated the communication mechanisms between the colony members. Particle
55 swarm optimization (PSO) [9][10] proposed by Eberhart and Kennedy in 1995 simulates a simplified

56 social model [11].

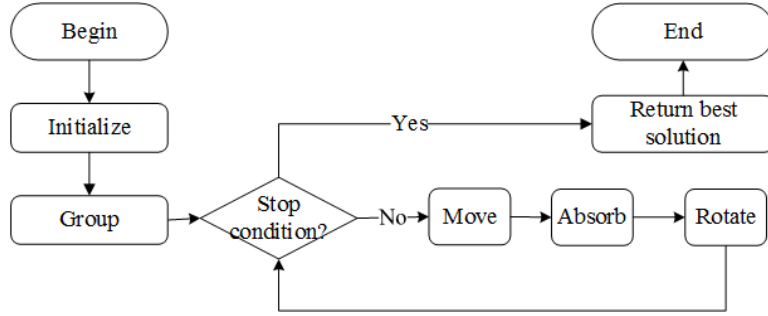
57 Furthermore, there has been an innovative CI algorithm boom over the last twenty years. In 2013,
58 Xing *et al.* [12] identified a vast amount of novel CI algorithms (more specifically, 134 in total) and
59 grouping them into four large classes, i.e., biology- (99 in total) [13-16], physics- (28 in total) [17-19],
60 chemistry- (5 in total) [20], and mathematics-based (2 in total) [21] CI algorithms. The core algorithm
61 concerned in this research is the gravitation field algorithm (GFA), which belongs to the second class
62 (physics-based CI). GFA [22-24] proposed by Zheng *et al.* in 2012 simulates the formation process of
63 planets based on the Solar Nebular Disk Model (SNDM) [25] in astronomy. Based on the original GFA,
64 we have developed an improved version of GFA called GFA-OD [26] (Optimal Detection). Almost all of
65 these innovative CI algorithms have good performance and some of them have been successfully applied
66 in many real-world optimization problems including unconstrained ones.

67 In this research, based on the original GFA and the earlier version of GFA-OD, we propose an
68 improved version of GFA, which is called Explosion Gravitation Field Algorithm (EGFA), and we
69 compare EGFA with popular approaches, including the original GFA, GA and PSO. More specifically,
70 in EGFA, we develop an improved strategy called Dust Sampling (DS) to locate the space that contains
71 the optimal solution(s) by initializing dust population randomly in a given problem search space, and this
72 makes the algorithm more efficient. Additionally, to improve the accuracy of solutions and decrease the
73 probability of the algorithm falling into local optima, an improved strategy named Explosion Operation
74 is introduced, the aim of which is to improve the performance of EGFA by generating new dust
75 population around center dust to replace the original dust. For implementing EGFA, we integrate two
76 processes: movement and rotation, and modify the formula for updating dust population. From the
77 experimental results on six complex unconstrained benchmark problems, we find that EGFA is superior
78 to the original GFA and two other classical optimization algorithms (GA and PSO) in terms of accuracy
79 and efficiency. In addition, further experiments show that EGFA outperforms the original GFA and k-
80 means on three real datasets. All the experimental results demonstrate the application potential of EGFA
81 in more complex problems.

82 **2. Explosion Gravitation Field Algorithm**

83 **2.1 The Original Gravitation Field Algorithm**

84 The original GFA was proposed in [23] as a novel nature-inspired heuristic search algorithm. The basic
 85 idea of GFA is to simulate the formation process of planets based on SNDM [25]. In GFA, all individuals
 86 can be mimicked as dust with mass, and each of them belongs to a certain group. In each group, the one
 87 with the biggest mass is regarded as the center dust and others are surrounding dust. Based on SNDM,
 88 each center dust attracts its surrounding dust by the gravitation field, and the field makes all surrounding
 89 dust move toward their center dust with heaviest mass. In addition, each dust has four characteristics:
 90 position, mass, group number, and a Boolean flag indicating whether it is a center. The position
 91 corresponds to a solution of the problem, the group number is initialized randomly, and the other two:
 92 mass and flag, are determined by the objective function. The flow chart of GFA is given in Fig.1. The
 93 details of GFA are summarized as follows, and all the parameters are set according to Zheng *et al.* [23].



94
95 Fig. 1 The workflow of GFA
96

- 97 ● Step 1: generate n dusts $D_i (i=1,2,\dots,n)$ randomly distributed in the mass function domain
 98 bound to establish the initial solution space when all parameters are set, where the position of the
 99 i th dust is defined by Eq. (1).

100
$$X_i = (x_{i,1}, x_{i,2}, \dots, x_{i,k}, \dots, x_{i,d}), \quad i = 1, 2, \dots, N \quad (1)$$

101 In the above $x_{i,k}$ is the position of the i th dust in the k th dimension, and d is the number of
 102 dimensions of search space. In addition, every dust (solution) D_i is assigned a mass M_i , whose values
 103 are calculated based on the objective function or the benchmark function.

- 104 ● Step 2: divide the search space into several subspaces randomly. Each dust D_i is allocated to a

105 subspace (called a group in GFA) randomly and the group number G_i is calculated by Eq. (2),
 106 where *ceil* is a function that rounds the elements to the nearest integers greater than or equal to it.
 107 In each subspace, the dust with the heaviest mass is called the center dust and we assign its flag
 108 $F_i = 1$, and others are the surrounding dusts and we assign their flags as $F_i = 0$.

$$109 \quad G_i = \text{ceil}(\text{rand}[0,1] * \text{group_num}) \quad (2)$$

110 ● Step 3: move dust. Every surrounding dust move toward its center dust and the center dust remain
 111 stationary. The pace of movement is determined by Eq. (3).

$$112 \quad \text{Pace}_i = w \times \text{dis}_i, \quad (3)$$

113 where dis_i is the Euclidean distance between the moving surrounding dust and its center dust in
 114 [22] and is also defined as the difference between two vector variables in [23]. w is a weight
 115 value for distance [22].

116 ● Step 4: absorb dust. Some surrounding dusts which are close to their center dust enough are
 117 absorbed by their center dust and therefore eliminated from the initial search space for increasing
 118 the convergence speed of GFA.

119 ● Step 5: perform rotation operation. The introduction of Rotation Operator in [23] is to push the
 120 surrounding dusts away from their center dust, which can decrease the probability of dusts falling
 121 into local optima to some extent. The rotation direction is not the original forward direction, but it
 122 could be any possible random direction. To prevent the surrounding dusts from being pushed too
 123 far, the pace is no greater than the max pace withdraw_{\max} , which is defined by Eq. (4).

$$124 \quad \text{withdraw}_{\max} = 2 \times \text{dis} \times 0.0618 \quad (4)$$

125 The rotation operation is performed with the probability of Rotation Factor (RF) [23]. The value of
 126 RF is defined in Eq. (5).

$$127 \quad \text{factor}^{t+1} = \begin{cases} \text{factor}_{\max}, & \text{factor}^t \geq \text{factor}_{\max} - 0.03 \\ \text{factor}^t + 0.03, & \text{factor}^t < \text{factor}_{\max} - 0.03 \end{cases}, \quad (5)$$

128 where factor^{t+1} is the RF in the $(t+1)$ th iteration, factor_{\max} is the max value of RF. This value
 129 cannot be too large, and it will gradually increase along with the running process of the algorithm.
 130 In [23], $\text{factor}^0 = 0$, and after several iterations, the RF will reach its max value and remain
 131 unchanged.

132 ● Step 6: check the termination criterion. If the algorithm does not meet the stopping condition, GFA
133 will go to Step 3, otherwise, the algorithm will terminate.

Algorithm 1: GFA

```
1. initialdusts ← Initialize(bound, N, targetFun, M) //initial
2. [groupdusts, center] ← Group(initialdusts, G) //divide search space into groups
3. dusts ← groupdusts
4. while the stop condition is not met do
5.   movedusts ← Move(dusts, center, targetFun) //move
6.   absorbdusts ← Absorb(movedusts) //absorb
7.   rotatedusts ← Rotate(absorbdusts, targetFun) //rotate
8.   dusts ← rotatedusts
9. end
10. return best solution(s)
```

134 According to the basic steps of GFA described above, every dust can be represented by a quadruple
135 (X_i, M_i, G_i, F_i) , and the pseudo-code of the original GFA model is given in **Algorithm 1**, where N is
136 the size of the population, M is the number of iterations; G is the number of groups; and $bound$ is a
137 $d * 2$ matrix that records the boundary of search space. The first five steps of GFA previously mentioned
138 correspond to five procedures: ‘**Initialize**’, ‘**Group**’, ‘**Move**’, ‘**Absorb**’ and ‘**Rotate**’. It is obvious that
139 these five procedures have a computational complexity of $O(N)$, where N is the size of population,
140 and the whole GFA model requires an $O(M \times N)$ of time complexity since the number of iteration M
141 is one of the termination criteria.

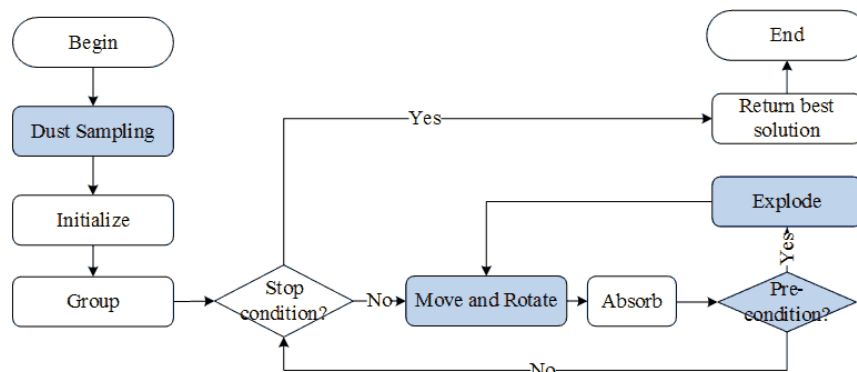
142 The original GFA has been used to optimize several unconstrained optimization problems, and it
143 has demonstrated excellent performance in these problems. It was reported that GFA was very effective
144 to find approximate optimal solutions for several unconstrained optimization problems. However, there
145 are still some limitations for the original GFA, as shown below:

146 1) The solutions that GFA obtains are particularly sensitive to the initial population. It is reported
147 that the accuracy of solution is closely related to the initial population [26]. GFA tends to find a solution
148 that usually could not meet the accuracy requirement of problems in given running time in many real-
149 world problems if the initial dust population is generated randomly in the whole search space.

150 2) GFA may be in stagnation behavior easily during the iteration process because of falling into
151 local optima, and in these cases the algorithm will return a local optimal solution or even a worse one if
152 there is no appropriate strategy to jump out from the bad results.

153 **2.2. Explosion Gravitation Field Algorithm**

154 To address the limitations of GFA presented above, an improved Explosion Gravitation Field Algorithm
155 (EGFA) was proposed with three aspects of improvement: two of them are two improved strategies called
156 Dust Sampling (DS) and Explosion Operation in this research, and another one is the integration of the
157 two processes: move and rotate. DS is performed when the parameter setting is completed and it is no
158 longer performed once this process is over. It can efficiently locate a small enough search space which
159 more likely contains the optimal solution(s). The second aspect of improvement, the Explosion Operation,
160 is performed once one of the pre-specified conditions is met. The Explosion Operation is used to jump
161 out from a local optimal solution with a certain probability and therefore improve the accuracy of
162 solutions. Furthermore, to simplify the process of EGFA, there is another improvement: the processes of
163 movement and rotation are integrated, and the formula for updating the dust population is modified. The
164 whole core aspects of improvement in EGFA are described below and the workflow of EGFA is given in
165 Fig. 2.



166

167

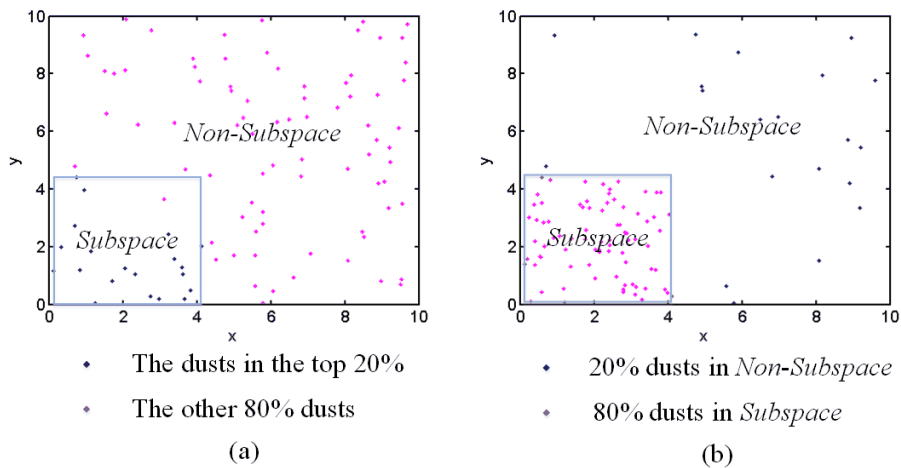
Fig. 2 The workflow of EGFA

168 **2.2.1 Subspace location by dust sampling**

169 As mentioned in Section 2.1, the original GFA starts with dust population being initialized randomly in
170 a giving search space, this makes it a long iterative process to find a solution that meets the accuracy
171 requirement for a given problem. The solution that the original GFA finds may be a suboptimal one
172 whose accuracy could not be comparable to the solutions found by other classical metaheuristic search
173 algorithms, such as GA and PSO. Therefore, to improve the accuracy and shorten the overall running
174 time, we proposed a subspace location strategy named Dust Sampling (DS). The DS operator is not only

175 an important improvement in this research but also the core component of EGFA. The task of DS is to
 176 efficiently locate a small enough search space which more likely contains the optimal solution(s), and
 177 this shares some similarities with our original Optimal Detection (OD) operator [26]. The readers are
 178 referred to [26] for more details about the original OD operation.

179 The DS operation begins with all dusts being initialized randomly in the given search space of a
 180 problem, then as shown in Fig. 3.(a), the dusts in the top 20% of the population are selected to calculate
 181 the boundary of the ‘*Subspace*’, and the solution space containing the other 80% of dusts population is
 182 named ‘*Non-Subspace*’. The top 20% of dusts are selected based on their mass values calculated from
 183 the mass function, similar with the fitness values in GA and PSO. In the next DS, 80% of dusts are
 184 generated in the ‘*Subspace*’ and just 20% of the dusts are generated in the ‘*Non-Subspace*’ randomly,
 185 which is illustrated in Fig. 3.(b). This process will be executed several times until the ‘*Subspace*’ is small
 186 enough. According to the above description, the pseudo-code of DS can be concluded in **Algorithm 2**.



187
 188 Fig. 3 The distribution of the dusts in *Subspace* and *Non-Subspace*

189 In [26], the algorithm can obtain a correct solution only when the hypothesis that the ‘*Subspace*’
 190 found by OD contains the optimal solution(s) is valid. If OD finds a wrong ‘*Subspace*’, the algorithm
 191 can only obtain a suboptimal solution. To overcome this limitation and decrease the probability of getting
 192 a suboptimal solution, every dust generated by DS is located in the ‘*Non-Subspace*’ with the probability
 193 of 20%. Even if the ‘*Subspace*’ does not contain the optimal solution(s), DS will still have a chance to
 194 locate the position of optimal solution(s) in the ‘*Non-Subspace*’. The choice of 20% and 80% when
 195 dividing the dusts for subspace and non-subspace is based on the Pareto principle, and in the future work
 196 we could further explore whether and how we can further improve this choice with better division.

197 The reason for the DS operator shortening the running time is because the main loop of the

198 algorithm just needs to find the optimal in a smaller search space and avoid a long iterative process to
 199 find a solution that meets the accuracy requirement, and this shares some similarities with our original
 200 OD [26]. However, a key to the original OD is that users have to specify the number of iterations and the
 201 size of the dusts population for the process to acquire a satisfactory ‘*Subspace*’, but it may be difficult
 202 for inexperienced users to provide such appropriate values. If the values are too large, the OD operation
 203 may take a long time, which lead to the decrease of the algorithm efficiency; if the value is too small, the
 204 algorithm may not be able to find a solution that meets the requirement of accuracy. The DS overcomes
 205 the above limitation and simplify the process of parameter setting for users. This operation provides
 206 default values for the number of iterations and the size of dusts population, according to the dimensions
 207 of the given problems. Specifically, the operation provides larger values for the complex problems with
 208 larger number of dimensions and provides smaller values for the uncomplex problems with smaller
 209 number of dimensions. The number of iterations and the size of population for the process increase with
 210 the increase of the complexity of a given problem. Let M_1 be the number of iterations for this process,
 211 and it is set as the stopping condition; if N is the size of population and d is the number of dimensions
 212 of the given problem, the process requires $O(M_1 \times N \times d)$ time complexity.

Algorithm 2: Subspace location by dust sampling

1. $Subspace \leftarrow Solution\ Space$;
2. $Non-Subspace \leftarrow Solution\ Space - Subspace$;
3. **While** the stopping conditions are not met **do**
4. **if** $Non-Subspace$ is null **then**
5. generating all dust population in the $Subspace$;
6. **else**
7. generating 80% dust population in the $Subspace$;
8. generating 20% dust population in the $Non-Subspace$;
9. **end**
10. picking up the top 20% of the population and calculating the boundary of the subspace;
11. $Subspace \leftarrow$ the boundary of the subspace;
12. $Non-Subspace \leftarrow Solution\ space - Subspace$;
13. **end**

213 Obviously, the fact that the number of the iterations and the size of dust population do not need to
 214 be assigned by the users in DS, and this makes the algorithm more robust to problems of different
 215 complexity compared with the original OD operation.

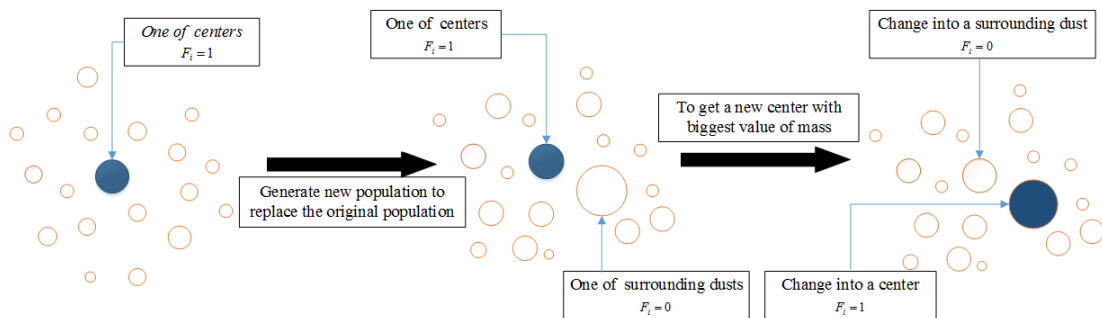
216 **2.2.2 Explosion Operation**

217 The algorithm may still fall into local optima or cannot find a solution that meets the accuracy
 218 requirement for the given problem if the ‘Subspace’ identified by **Algorithm 2** does not contain the
 219 actual optimal solution. Regarding this, we introduce the Explosion operation to decrease the probability
 220 of dust falling into local optima compared with the original GFA, GA and PSO. The algorithm will
 221 perform the explosion operation when one of the following conditions is triggered.

222 1) *The algorithm is in stagnation behavior.* The explosion operation will be executed since the
 223 solutions that the algorithm finds will not be better in the future iteration process.

224 2) *The size of population is less than a pre-specified threshold.* The explosion operation is needed
 225 since the solution is less likely to get better in this case.

226 When one of above two conditions is triggered, all dusts will be removed except the center dust in
 227 each group. Then the algorithm will perform the explosion operation and generate a new population to
 228 replace the original one. The generation of the new population is not random, and it uses the knowledge
 229 from the last population. The process of explosion for one group is illustrated in Fig. 4.



230

231

Fig. 4 One of the centers generate a new population to replace the original one

232

233 As shown in Fig. 4, the biggest blue dot with $F_i = 1$ in a group is the center dust and other dots
 234 are the surrounding dust with $F_i = 0$. Obviously, the task of Explosion Operation is to generate a new
 235 population around the center, and then attempt to find a better solution among the new population. The
 236 distribution of the new population is given by Eq. (5).

237
$$X_i^k = s \times (ub_k - lb_k) \times c \times \text{normrnd}[0,1] + X_{center_i}^k, k = 1, 2, \dots, d, \quad (5)$$

238 where d is the number of dimensions, s is a positive or negative sign generated randomly in a
 239 mathematical operation, ub_k and lb_k are the upper and lower bounds of the k th dimension in search

240 space. The Gaussian function $normrnd[0,1]$ determines how new dust will be distributed in the k -
 241 dimensional search space, where $0 < normrnd[0,1] < 1$, and the mean and standard deviation for the
 242 Gaussian function are 0.025, 0.25, respectively. The coefficient c determines the degree of aggregation
 243 for dusts in each group, where $0 < c < 1$. For each group, the less the value of c is, the more
 244 concentrated the distribution of the dust is; the larger the value of c is, the more dispersed the
 245 distribution of dust is.

246 The Explosion is performed when one of the following two conditions is triggered: (1) the algorithm
 247 is in the stagnation behavior, and (2) the size of population is less than a pre-specific threshold. Obviously,
 248 the best solution the algorithm gets must be one of the centers. Provided that the algorithm has found an
 249 approximate optimal solution and the size of the population has been less than the pre-specified threshold,
 250 it is reasonable to believe that the better solution exists near one of the center dusts with high probability
 251 and the algorithm needs more dusts to explore the search space. Thus, the above approach can be used
 252 to find a better solution and improve the accuracy of historical best solution quickly. Additionally, if the
 253 algorithm has been in stagnation behavior because of falling into local optima, the algorithm can jump
 254 out from the local optimal solution with the help of surrounding dusts far away from the center dust with
 255 a certain probability. Therefore, the explosion operator introduced in EGFA can also be used to prevent
 256 the algorithm from being in stagnation behavior.

Algorithm 3: Explode

```

1. for  $i = 1:C$  //C is the size of each group
2.   for  $j = 1:G$  //for each dust in a group
3.      $index \leftarrow (i-1)*G + j$ 
4.     for  $k = 1:d$  %for the  $k$ th demonstration
5.        $X_i^k \leftarrow s \times (ub_k - lb_k) \times c \times normrnd[0,1] + X_{center}^k$  //the position of new dust
6.     end
7.      $M_{index} \leftarrow f(X_{index})$  //7-9 generate new dust
8.      $G_{index} \leftarrow j$ 
9.      $F_{index} \leftarrow 0$ 
10.  end
11. end

```

257 Following the details about Explosion described above, the pseudo-code of one of the centers
 258 generating a new population to replace the original one is presented in **Algorithm 3**, which is the main
 259 part of Explosion operation. In **Algorithm 3**, G is the number of groups; N is the size of the
 260 population; C is the size of each group; $N = C \times G$; d is the number of dimensions of the search

261 space for a given problem. This process requires an overall of $O(C \times G \times d) = O(N \times d)$ computations.

262 Note that only $O(N)$ storage is required for this process.

263 2.2.3 The Main loop

264 EGFA proposed in this research is an improved version of GFA, which introduces the DS and Explosion
265 operations to improve the algorithm performance. In addition, to simplify the process of EGFA, we
266 integrate the process of movement and rotation, and modify the formula for iteration. As a result, any
267 dust D_i in a given search space is described by a quadruple $D_i = (X_i, M_i, G_i, F_i)$ and the new
268 generation for the next iteration in the EGFA can be determined by Eq. (6).

$$269 \quad X_i^{t+1} = X_i^t + Pace_i^t, \quad (6)$$

270 where $Pace_i^t$ and X_i^t are the current pace and position of dust D_i at time t , respectively, and

271 $Pace_i^t$ is determined by three components as follows:

$$272 \quad Pace_i^t = (w_1 * dis_i^t + w_2 * Ibest^t) * (1 - F_i) + w_3 * rand(1, d), \quad (7)$$

273 where d is the dimension of the search space, w_1, w_2, w_3 stands for the weight values of the three
274 parts, respectively, $w_1 > w_2 > 0$, $w_3 > 0$, $F_i \in \{0, 1\}$ (F_i is equal to 1 when D_i is a center, otherwise,
275 F_i is equal to 0).

276 ● The first component dis_i^t is the directional difference of the position between the moving
277 surrounding dust D_i and its center at time t , which is calculated by Eq. (8) in EGFA.

$$278 \quad dis_i^t = X_{center_{G_i}}^t - X_i^t, \quad (8)$$

279 Where X_i^t and $X_{center_{G_i}}^t$ are the position of dust D_i and its center at time t , respectively.

280 ● The second component $Ibest^t$ stands for the improvement vector of the global best's position at
281 time t , and it is calculated by Eq. (9).

$$282 \quad Ibest^t = X_{best}^t - X_{best}^{t-1}, \quad (9)$$

283 where X_{best}^t is the position of current global best dust and X_{best}^{t-1} is the stored position of the global
284 best dust from the last generation. The concept of global best in this manuscript is similar to the

285 concept of global best Artificial Bee Colony (ABC), and reader can refer to [27] for more details
 286 about the concept. The main objective of this component is to modify the representative point by
 287 taking into account global directional moves so that to attract the path going to optima and reduce
 288 the time for reaching the global optima.

289 ● The third component $rand(1, d)$ is a $1 \times d$ matrix and produces random movements for all dusts,
 290 including the surrounding dusts and their centers, like all the planets in the universe are always in
 291 motion. As a result, the centers in EGFA are no longer still, and they move randomly toward any
 292 possible direction like surrounding dusts, which could help find a better center and improve the
 293 diversity of the population.

294 Furthermore, dust recovery is another interesting topic with regards to EGFA due to the fact that
 295 dust may move outside the search space and should be returned. There are many possible dust recovery
 296 methods. A useful one adopted in EGFA is the reposition factor (Frep for short) [19], which plays an
 297 important role in EGFA's convergence. They are described in Eq. (10) and Eq. (11) as below.

$$298 \quad X_{i,k}^t = X_{k,\min} + \varepsilon (X_{i,k}^{t-1} - X_{k,\min}) \quad (10)$$

$$299 \quad X_{i,k}^t = X_{k,\max} - \varepsilon (X_{k,\max} - X_{i,k}^{t-1}) \quad (11)$$

300 where k is the current dimension; t is the current time step; i is the current dust index; and ε is
 301 a small positive number chosen by the user, typically 0.0005. EGFA uses Eq. (10) to reposition dimension
 302 of dust that have exceeded their minimum values, while Eq. (11) is used to reposition dimensions of dust
 303 that have exceeded their maximum values.

304 According to the above details of EGFA, the pseudo-code of the main steps of EGFA is given in
 305 **Algorithm 4**. In the above variable k is a monitor, which is employed to record the number of iterations
 306 of the algorithm being in stagnation behavior during the search process, variable '*bound*' gives the value
 307 range of X_i in all dimensions for each solution D_i , N is the size of population, G is the number
 308 of groups, d is the number of the dimensions of the search space.

309 The method '*DustSampling*' corresponds to the process of Dust Sampling presented in Section
 310 2.2.1 and stores the information of '*Subspace*' with the variable '*BestBound*'. The method
 311 '*MoveAndRotate*' integrates the process of movement and rotation and corresponds to Eq. (6) for
 312 iteration. The method '*Explode*' corresponds to the process of explosion described in Section 2.2.2 and
 313 there exists a very important threshold variable f_{th} in the method, which is usually proportional to the

314 number of the iterations. If the condition $k > f_{th}$ is met, the method '**Explode**' will be performed. The
315 method '**Initialize**', '**Group**', '**Absorb**' still corresponds to the same processes as in the original GFA.
316 The method '**GetCenters**' is used to get the center dust for each group and the method '**GetBest**' is
317 devoted to update the historical best solution. Let M_2 be the number of iterations for the main loop and
318 set as one of the stop conditions. Obviously, the methods '**Initial**', '**Group**', '**MoveAndRotate**', '**Absorb**',
319 '**GetCenters**' and '**GetBest**' just require $O(N)$ time complexity. Since '**DustSampling**' requires
320 $O(M_1 \times N \times d)$ time complexity, and '**Explode**' requires $O(N \times d)$ time complexity, the main loop of
321 EGFA require an overall of $O((M_1 + M_2) \times N \times d)$ time complexity. Note that only $O(N)$ space

Algorithm 4: EGFA

```

1.  $k=0$ 
2.  $bestBound \leftarrow \text{DustSampling}(N, bound, targetFun);$  //dust sampling
3.  $initialdusts \leftarrow \text{Initialize}(bestBound, N, targetFun)$  //initialisation
4.  $[groupdusts, center] \leftarrow \text{Group}(initialdusts, G)$  //group
5.  $dust \leftarrow groupdusts$ 
6. while the stop conditions are not met do
7.      $movedust \leftarrow \text{MoveAndRotate}(dust, center, targetFun);$  //move and rotate
8.      $absdust \leftarrow \text{Absorb}(center, movedust, bestBound);$  //absorb
9.      $dust \leftarrow absdust$ 
10.    if pre-condition is met then
11.         $[dust, k] \leftarrow \text{Explode}(k, dust, N, bound, targetFun, center);$  //explode
12.    end if
13.     $[center, dust] \leftarrow \text{GetCenters}(G, dust);$  //get the center dusts of each group
14.     $[best, k] \leftarrow \text{GetBest}(best, center, k);$  // the best dust
15. end
16. return optimal solution

```

322 complexity is required for EGFA.

323 The two strategies proposed in EGFA overcome the limitations of the original GFA. However, the
324 introduction of these two strategies is at the cost of running time. It is noted that DS avoids the long
325 iterative process and shortens the running time, although the time complexity has increased to
326 $O((M_1 + M_2) \times N \times d)$. Last but not least, to prove the capacity in theory, the research discusses the
327 convergence of EGFA in one-dimension simply in the supplementary material. As for the convergence
328 in higher dimensional search space, it is a part of research in future work.

3. Experiments

3.1 Experiments on Benchmark problems

To assess the performance of EGFA proposed in this research, the following six benchmark unconstrained optimization problems in Table 1 are chosen, which are used to test the accuracy, running time of our algorithm with problems of different dimensions. At the same time, this series of classical test problems are also solved by the original GFA, GA and PSO to compare with EGFA. 100 trials of each algorithm are performed for solving these six benchmark problems, and we choose the mean value, the median value, the mean squared error and the Standard Deviation of solutions to evaluate the performance of the four algorithms. Finally, we present the experimental results and the discussions upon these results.

3.1.1 Benchmark problems and performance evaluation

The functions listed in Table 1 are some of the most commonly used functions used to assess the performance of unconstrained optimization algorithms. These benchmark problems are chosen from a number of significant past studies in unconstrained optimization. The functions [28] are known widely as the Sphere, Griewangk, Ackley, Zakharov, Rotated Hyper-Ellipsoid and Levy function, and they can be scaled to any number of variables (dimensions). Table 1 shows the domain, the objective function, and the global minimum for every benchmark problem. Additionally, the six benchmark problems have the same global minimum value $f(x^*)$, and the global minimum values of these six problems are equal to zero when the variables are equal to zero or one, regardless of the number of variables. The Zakharov, Sphere, and Rotated Hyper-Ellipsoid functions are continuous, convex, unimodal, and multidimensional. The first one is plate-shaped and the latter two are Bowl-Shaped in their two-dimensional forms. The others are multimodal, multidimensional, with a large number of local optima.

Table 1

The benchmark problems for testing EGFA, GFA, GA and PSO

Name	Variable ranges	Objective function	Optima
Sphere	$x_i \in [-50, 50]$	$f(x) = \sum_{i=1}^d x_i^2$	$x^* = (0, \dots, 0)$ $f(x^*) = 0$

Griewangk	$x_i \in [-5, 5]$	$f(x) = \sum_{i=1}^d \frac{x_i^2}{4000} - \prod_{i=1}^d \cos\left(\frac{x_i}{\sqrt{i}}\right) + 1$	$x^* = (0, \dots, 0)$ $f(x^*) = 0$
Ackley	$x_i \in [-50, 50]$	$f(x) = 20 + e - 20e^{\left[-0.2\sqrt{\frac{1}{d}\sum_{i=1}^d x_i^2}\right]} - e^{\left[\frac{1}{d}\sum_{i=1}^d \cos(2\pi x_i)\right]}$	$x^* = (0, \dots, 0)$ $f(x^*) = 0$
Zakharov	$x_i \in [-10, 10]$	$f(x) = \sum_{i=1}^d x_i^2 + \left(\sum_{i=1}^d 0.5ix_i\right)^2 + \left(\sum_{i=1}^d 0.5ix_i\right)^4$	$x^* = (0, \dots, 0)$ $f(x^*) = 0$
Rotated Hyper-Ellipsoid	$x_i \in [-50, 50]$	$f(x) = \sum_{i=1}^d \sum_{j=1}^i x_j^2$	$x^* = (0, \dots, 0)$ $f(x^*) = 0$
Levy	$x_i \in [-10, 10]$	$f(x) = \sin^2(\pi w_1) + \sum_{i=1}^{d-1} (w_i - 1)^2 [1 + 10 \sin^2(\pi w_i + 1)] + (w_d - 1)^2 [1 + \sin^2(2\pi w_d)]$ where, $w_i = 1 + \frac{x_i - 1}{4}$	$x^* = (1, \dots, 1)$ $f(x^*) = 0$

353 To investigate the accuracy and efficiency of EGFA, we choose four common performance metrics
354 for evaluating the performance of EGFA in comparison with the original GFA and two other classical
355 computational intelligence algorithms, i.e., GA and PSO. Four performance metrics are described as
356 follows:

- 357 1) The mean value of solutions that are found by the four algorithms for 100 different trials.
358 2) The median value of solutions that are found by the four algorithms for 100 different trials.
359 3) The Mean squared error (MSE) [29]: it has the general definition as in Eq. (12), where n is the
360 number of tests, $f(x_i)$ is the solution of i th run and $f_{opt}(x)$ is the true global minimum. Obviously,
361 the lower the Mean squared error (MSE) is, the better performance the algorithm has.

362
$$MSE = \frac{1}{n} \sum_{i=1}^n (f(x_i) - f_{opt}(x))^2, \quad (12)$$

- 363 4) The Standard Deviation (STD) [30]: it has the general definition as in Eq. (13), where n is the
364 number of tests, $f(x_i)$ is the solution of i th run and $\overline{f(x)}$ is the mean of all $f(x_i)$. Same as the
365 Mean squared error (MSE), the lower the Standard Deviation (STD) is, the better performance the
366 algorithm has.

367
$$STD = \sqrt{\frac{1}{n-1} \sum_{i=1}^n (f(x_i) - \overline{f(x)})^2}, \quad (13)$$

368 The mean value, the median value and the Mean squared error (MSE) are devoted to evaluate the

369 accuracy of solutions that are obtained by four different algorithms. The Standard Deviation (STD) is
 370 employed to measure the stability of the performance for the four test algorithms.

371 **3.1.2 Parameter settings**

372 The parameters and their values for the four algorithms are given in Table 2. The size of population is set
 373 as $100*d$, where d is the number of dimensions of a given search space. Moreover, $d = 2,3,5,10,20$
 374 has been tested in this research. The maximum number of iterations is set $200*d$ for the four
 375 algorithms to control their running time in the same dimension. The number of groups is just set as 3 for
 376 EGFA and the original GFA to ensure multi-centers in this research. The parameter TolFun is the average
 377 change in value of the fitness function or mass function and it is changed from the default value of $1.0e-$
 378 6 to $1.0e-30$ to ensure that the optimal solution they acquire is accurate enough.

379
 380 Table 2

381 The parameter settings for EGFA, GFA, GA and PSO

Parameters setting	EGFA	GFA	GA	PSO
Population size	$100*d$	$100*d$	$100*d$	$100*d$
The Max number iterations	$200*d$	$200*d$	$200*d$	$200*d$
The number of group	3	3	-	-
TolFun	$1.0e-30$	$1.0e-30$	$1.0e-30$	$1.0e-30$

382
 383 In this research, every test problem shown in Table 1 is scaled to different number of variables, whose
 384 value range of each dimension is also set as in Table 1. The basic parameters of each algorithm are set as
 385 in Table 2. Four performance metrics, the mean value, the median value, MSE, and STD, are employed
 386 to measure the accuracy, efficiency of each algorithm in given running time. In this study, we do not
 387 make any systematic attempt to find the best parameters for EGFA and just focus on the accuracy of each
 388 algorithm in given running time. The higher accuracy of the optimal solution is, the better the
 389 performance the algorithm has.

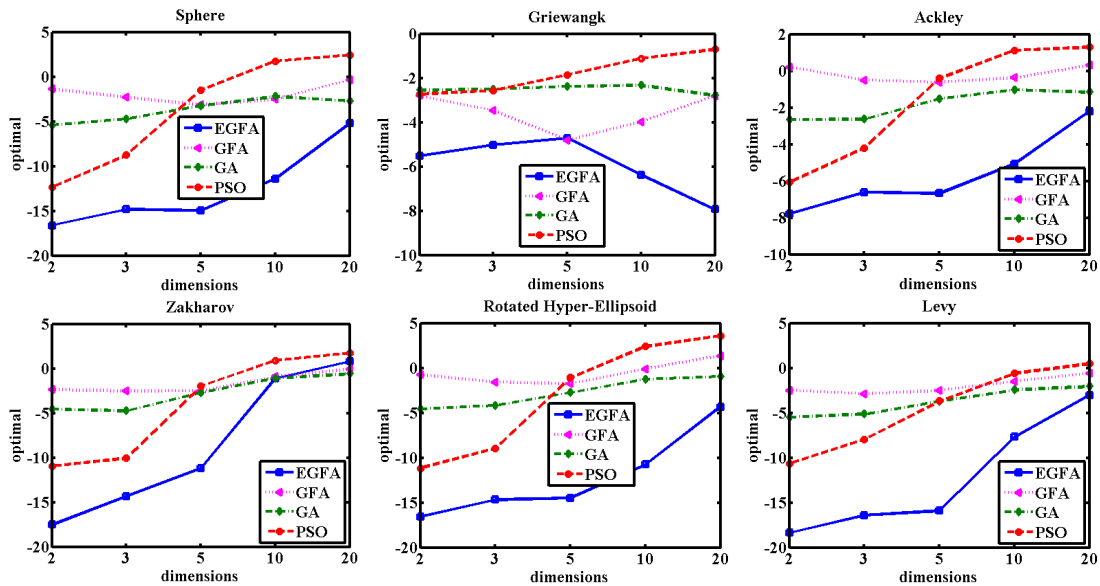
390 **3.1.3 Parametric statistical test**

391 To compare the performance of EGFA, GFA, GA and PSO on unconstrained optimization problems with
 392 different numbers of dimensions in given running time, six test problems with $2,3,5,10,20$ dimensions

393 are used. The comparisons of four algorithms: EGFA, GFA, GA and PSO on the six test problems in
 394 mean value, median value, MSE and STD are shown in Figs. 5~8. More specifically, the results of Figs.
 395 5~8 are the mean value, median value, MSE and the STD of 100 trials, which the size of the population
 396 is set as $100 * d$, where d is the number of dimensions and $d = 2, 3, 5, 10, 20$, the iterations for EGFA,
 397 GFA, GA and PSO is set as $200 * d$.

398 Fig. 5 shows that EGFA achieves better performance in terms of mean value than GFA, GA and
 399 PSO; Fig. 6 shows that EGFA achieves better performance in terms of median value than GFA, GA and
 400 PSO. Especially in search space of low dimensions, we can see that EGFA outperforms GFA, GA and
 401 PSO in terms of accuracy. Fig. 7 shows that the solution obtained by EGFA has less value of the MSE
 402 than GFA, GA and PSO, therefore we can see that EGFA has less error than the other three algorithms.
 403 Fig. 8 demonstrates that EGFA has more stable performance compared with GFA, GA and PSO since
 404 EGFA has the least value of STD among the four algorithms. In addition, the accuracy of solutions
 405 obtained by EGFA will decrease with the increase of the dimensions of search space like PSO, but EGFA
 406 has better accuracy than PSO as shown in Figs. 5-8.

407



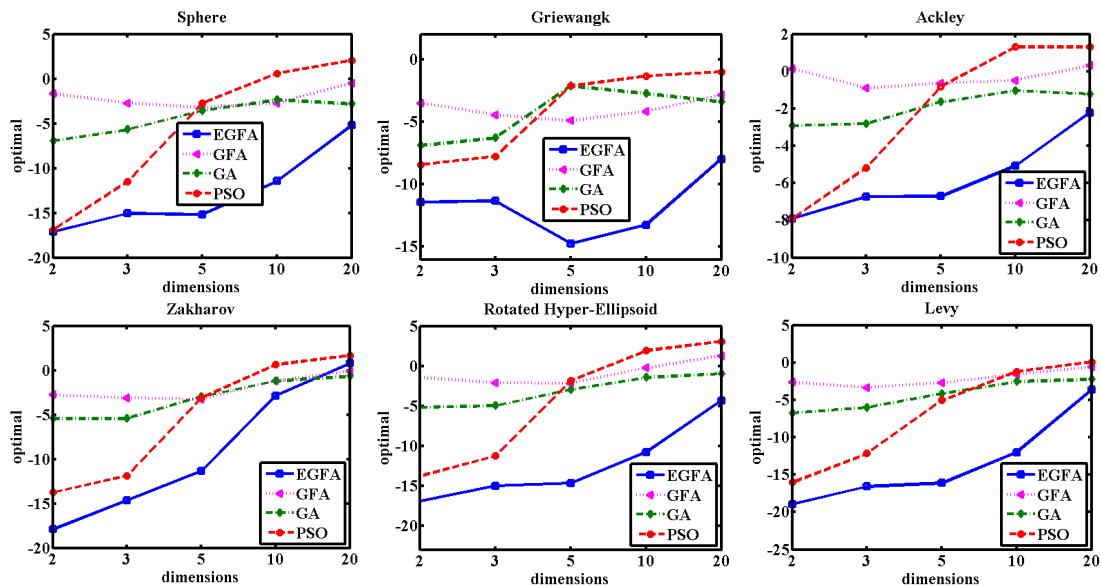
408

Fig. 5. A Comparison of EGFA, GFA, GA and PSO in $\log_{10}(\text{mean})$ with 2,3,5,10,20 dimensions

409

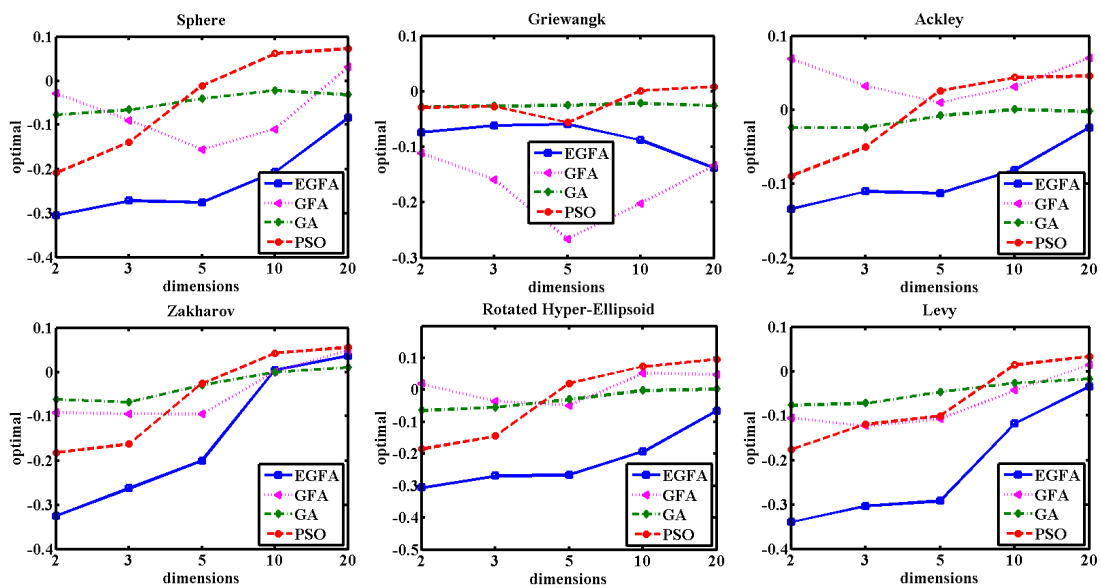
410 Besides the accuracy, the running time is another very important factor that we should consider in
 411 order to measure the efficiency of an algorithm. It is obvious that the introduction of DS and Explosion
 412 operations are at cost of time, but the optimal space the DS acquires can help to decrease the number of

413 iterations and shorten the overall running time. The average running time of the four algorithms for 100
 414 trials on the six test problems with the number of dimensions $d = 2, 3, 5, 10, 20$ is demonstrated in Table
 415 3 and Fig. 9. Table 3 shows that the performance of the four algorithms is controlled in similar running
 416 time, when they are executed on the same problem in same dimension. Fig. 9 shows that EGFA has the
 417 best efficiency for solving the six test problems in some content. And Fig. 9 also shows that the running
 418 time of the four algorithms on the test problems increases exponentially with the increase of the
 419 dimensions. All experiments were implemented on a PC (i5-4200M, 8GB, Windows 7, Matlab R2014a).
 420

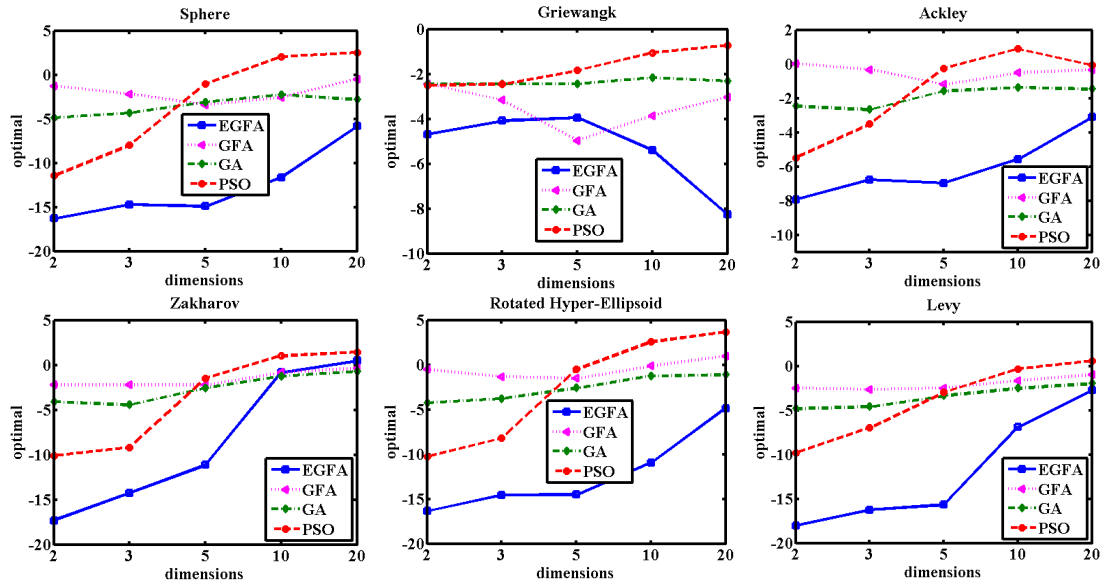


421 Fig. 6. A Comparison of EGFA, GFA, GA and PSO in $\log_{10}(\text{median})$ with 2,3,5,10,20 dimensions

422



423 Fig. 7. A Comparison of EGFA, GFA, GA and PSO in $\log_{10}(\text{MSE})$ with 2,3,5,10,20 dimensions



424 Fig. 8. A Comparison of EGFA, GFA, GA and PSO in $\log_{10}(\text{STD})$ value with 2,3,5,10,20 dimensions

425

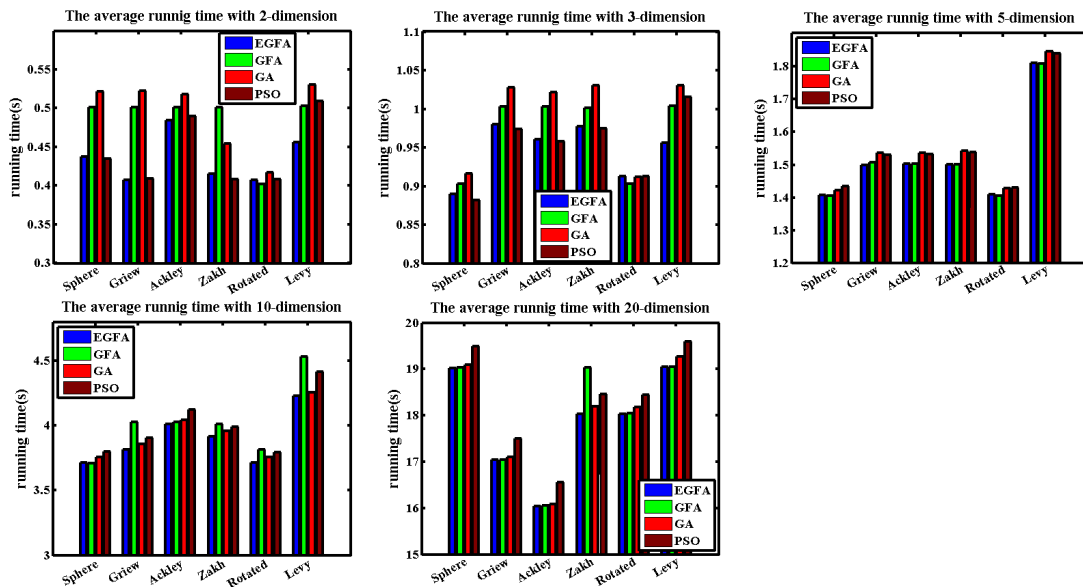
426 Table 3

427 The average running time for 100 trials of six benchmark functions with dimension $d=2,3,5,10,20$

Benchmark	Function	2	3	5	10	20
Sphere	EGFA	0.4381s	0.8898s	1.4093s	3.7177s	19.0255s
	GFA	0.5013s	0.9028s	1.4056s	3.7115s	19.0313s
	GA	0.5218s	0.9164s	1.4218s	3.7560s	19.0874s
	PSO	0.4315s	0.8820s	1.4350s	3.7997s	19.4872s
Griewangk	EGFA	0.4074s	0.9803s	1.4993s	3.8174s	17.0395s
	GFA	0.5018s	1.0027s	1.5081s	4.0279s	17.0497s
	GA	0.5225s	1.0276s	1.5361s	3.8566s	17.0977s
	PSO	0.4098s	0.9739s	1.5305s	3.9028s	17.4997s
Ackley	EGFA	0.4839s	0.9627s	1.5041s	4.0129s	16.0337s
	GFA	0.5015s	1.0029s	1.5077s	4.0257s	16.0513s
	GA	0.5186s	1.0221s	1.5372s	4.0426s	16.0824s
	PSO	0.4897s	0.9575s	1.5327s	4.1212s	16.5579s
Zakharov	EGFA	0.4158s	0.9771s	1.5019s	3.9152s	18.0285s
	GFA	0.5013s	1.0014s	1.5345s	4.0141s	19.0296s
	GA	0.4544s	1.0304s	1.5418s	3.9605s	18.1944s
	PSO	0.4081s	0.9750s	1.5384s	3.9908s	18.4605s
Rotated Hyper-Ellipsoid	EGFA	0.4074s	0.9125s	1.3598s	3.7141s	18.0331s
	GFA	0.4021s	0.9031s	1.4052s	3.8168s	18.0481s
	GA	0.4169s	0.9119s	1.4285s	3.7592s	18.1806s
	PSO	0.4080s	0.9125s	1.4314s	3.7941s	18.4442s
Levy	EGFA	0.4558s	0.9560s	1.8099s	4.2267s	19.0550s
	GFA	0.5028s	1.0036s	1.8073s	4.5340s	20.0777s

GA	0.5303s	1.0303s	1.8448s	4.2536s	19.2646s
PSO	0.5090s	1.0156s	1.8381s	4.4143s	19.5955s

428



429 Fig. 9 The average running time for 100 trials of six benchmark functions with dimension $d = 2, 3, 5, 10, 20$

430 **3.1.4 Non-parametric statistical test**

431 To further verify the conclusion drawn from the part of parametric statistical test in Section 3.2.1,
 432 following [31] we use a non-parametric statistical method, called the Wilcoxon test [32] [33], to compare
 433 the performance of EGFA, GFA, GA and PSO. Table 4 shows the Wilcoxon test results of the 100 trials
 434 for the four algorithms on the six test problems, and readers can refer to [34] for more details about how
 435 to use the Wilcoxon test to compare different metaheuristic algorithms in detail.

436 In the Wilcoxon test presented in Table 4, we set the significance level p to be 0.05 ($p = 0.05$) and
 437 use the two-tailed hypothesis because the settings of the both are the most commonly. We have 100 trials
 438 (which means the sample size $N = 100$) for the four algorithms on the six test problems in 2, 3, 5, 10, 20
 439 dimensions, and calculate both p -value and h -value to compare the performance of each pair of the
 440 algorithms. If the p -value is less than the significance level ($p = 0.05$) and $h = 1$, the results indicate
 441 that there is a significant difference between the performance of the two algorithms. Otherwise, it
 442 indicates that there is not enough evidence to verify the significant difference between the performance
 443 of the two algorithms

444 Since we know that the performance of the two algorithms is significantly different, to further
 445 determine which algorithm performs better we will focus on the value of the rank sum for the former

446 algorithm $\sum R_1$ and the latter algorithm $\sum R_2$, that is, if $\sum R_1$ is less than $\sum R_2$, it indicates that
 447 the former algorithm outperforms the latter one, otherwise, the latter one outperforms the former one.

448 For each cell in Table 4, the first value is the p -value and is representative of the probability that the
 449 results for the two algorithms obey the same distribution. The second value is the h -value. If the h -value
 450 is equal to 1 ($h = 1$), it indicates that the performance of the two algorithms is significantly different. If
 451 there is no significant difference between the two algorithms, the h -value is equal to 0 ($h = 0$). A ‘-’ sign
 452 means that the former one outperforms the latter one ($\sum R_1 < \sum R_2$). Similarly, a ‘+’ sign means
 453 $\sum R_1 > \sum R_2$ and indicates that the latter algorithm outperforms the former one. For instance, from the
 454 three rows about the Rotated Hyper-Ellipsoid problem in Table 4, all the p -values are smaller than the
 455 significance level ($p = 0.05$), h -value is 1, and the ‘-’ sign demonstrates that EGFA outperforms GFA,
 456 GA and PSO at $p = 0.05$ on the Rotated Hyper-Ellipsoid problem in 2,3,5,10,20 dimensions because
 457 of $\sum R_1 < \sum R_2$. The results are consistent with the distribution of the results obtained by the four
 458 algorithms on 100 trials presented in Fig. 10. Fig. 11 presents the distribution of the results for the four
 459 algorithms on Rotated Hyper-Ellipsoid in 20-dimensional search space in detail, which corresponds to
 460 the cell ‘1.1720e-16/1/-’, ‘2.5621e-34/1/-’ and ‘2.1609e-23/1/-’ in the Table 4.

461 From the results presented in Table 4, as well as in Fig. 10 and Fig. 11, we can see that results
 462 obtained from the Wilcoxon test confirm the conclusions drawn from Section 3.2.1, that is, EGFA
 463 outperforms GFA, GA and PSO on all six test problems in the overall level.

464

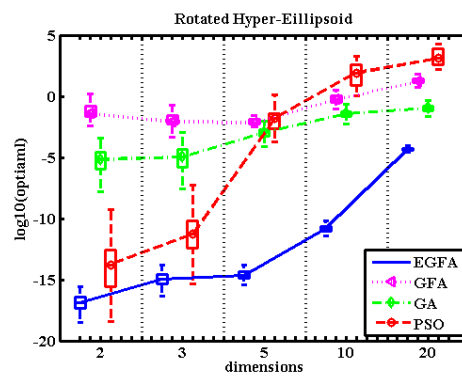
465 Table 4

466 Results of Wilcoxon rank sum test for statistically significance level at $p = 0.05$ for optimal solution over 100
 467 runs on benchmark functions for 2,3,5,10,20 dimensions

Benchmark Function		2	3	5	10	20
		p/h/zval				
Sphere	EGFA vs GFA	3.0199e-11/1/-	3.0199e-11/1/-	3.0199e-11/1/-	3.0199e-11/1/-	3.0199e-11/1/-
	EGFA vs GA	2.5621e-34/1/-	2.5621e-34 /1/-	2.5621e-34 /1/-	2.5621e-34 /1/-	2.5621e-34/1/-
	EGFA vs PSO	0.2241 /0/-	4.9856e-29 /1/-	2.5621e-34 /1/-	2.5621e-34 /1/-	2.5621e-34 /1/-
Ackley	EGFA vs GFA	3.0199e-11/1/-	3.0199e-11/1/-	3.0199e-11/1/-	3.0199e-11/1/-	3.0199e-11/1/-
	EGFA vs GA	2.5621e-34/1/-	2.5621e-34/1/-	2.5621e-34/1/-	2.5621e-34/1/-	2.5621e-34/1/-
	EGFA vs PSO	0.7022/0/-	2.2224e-27/1/-	2.5621e-34/1/-	2.5621e-34/1/-	2.5621e-34 /1/-
Griewangk	EGFA vs GFA	3.0199e-11/1/-	3.1589e-10/1/-	1.0601e-07/1/-	3.1589e-10/1/-	3.0199e-11/1/-

	EGFA vs GA	3.7064e-23/1/-	3.2066e-29/1/-	1.3673e-31/1/-	9.6788e-31/1/-	2.5621e-34/1/-
	EGFA vs PSO	1.1068e-07/1/-	4.4804e-09/1/-	2.5074e-33/1/-	6.6802e-34/1/-	2.5621e-34/1/-
Levy	EGFA vs GFA	3.0199e-11/1/-	3.0199e-11/1/-	3.0199e-11/1/-	2.9543e-11/1/-	3.0199e-11/1/-
	EGFA vs GA	2.5621e-34/1/-	2.5621e-34/1/-	2.5621e-34/1/-	2.5306e-34/1/-	1.4447e-22/1/-
	EGFA vs PSO	8.2778e-22/1/-	3.6728e-34/1/-	2.5616e-34/1/-	2.5306e-34/1/-	2.5621e-34/1/-
Rotated Hyper-	EGFA vs GFA	3.0199e-11/1/-	3.0199e-11/1/-	3.0199e-11/1/-	3.0199e-11/1/-	1.1720e-16/1/-
Ellipsoid	EGFA vs GA	2.5621e-34/1/-	2.5621e-34/1/-	2.5621e-34/1/-	2.5621e-34/1/-	2.5621e-34/1/-
	EGFA vs PSO	2.1609e-23/1/-	5.7156e-30/1/-	2.5621e-34/1/-	2.5621e-34/1/-	2.5621e-34/1/-
Zakharov	EGFA vs GFA	3.0199e-11/1/-	3.0199e-11/1/-	8.1527e-11/1/-	9.2113e-05/1/-	6.1210e-10/1/+
	EGFA vs GA	2.5621e-34/1/-	2.5621e-34/1/-	3.6728e-34/1/-	5.3312e-12/1/-	3.0679e-34/1/+
	EGFA vs PSO	6.9521e-30/1/-	1.3281e-21/1/-	5.4201e-34/1/-	5.4201e-34/1/-	2.5621e-34/1/-

468



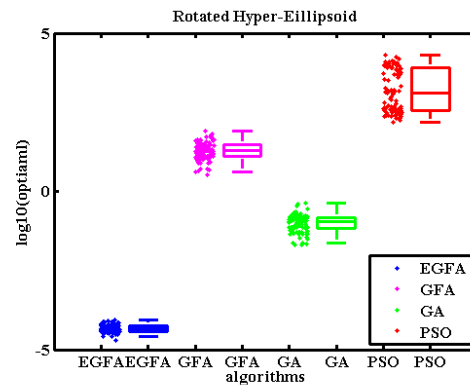
469

470 Fig. 10 The distribution of the results for EGFA, GFA, GA and PSO on Rotated Hyper-Ellipsoid in 2,3,5,10,20

471

dimensions

472



473

474 Fig. 11 The distribution of the results for EGFA, GFA, GA and PSO on Rotated Hyper-Ellipsoid in 20 dimensions

475 3.2 Experiments on real datasets

476 Clustering is an important data mining task and it has been explored extensively in different application

477 areas. To assess the excellent performance of the model in real world applications, the GFA and EGFA

478 are applied to clustering problems in this research so that we can explore the application potential of GFA
479 and EGFA on real world problems.

480 **3.2.1 The Encoding of cluster centroid vector**

481 In this research, we applied GFA and EGFA to clustering, based on the original idea of k-means. The
482 process of clustering can be regarded as the unconstrained optimization problems since its objective
483 function is constrained. In the context of clustering, a single dust represents the K cluster centroid
484 vectors. That is, each dust \vec{X}_i is constructed in the form of Eq. (14),

$$485 \quad \vec{X}_i = (x_{i,1}, x_{i,2} \cdots x_{i,j} \cdots x_{i,K}) , \quad (14)$$

486 where $x_{i,j}$ refers to the j -th cluster centroid vector of the i -th dust. Therefore, the dust population
487 represents candidate cluster centroid vectors.

488 The mass function of individual is measured as Eq. (15) [35], which is similar to the objective in k-
489 means clustering algorithm.

$$490 \quad \max \text{massFunction} = - \sum_{i=1}^K \sum_{s \in C_i} \left\| s - \vec{m}_i \right\|_2^2 , \quad (15)$$

491 where \vec{m}_i is the i -th cluster centroid vector, s is the i -th sample that belongs to the cluster C_i , and
492 K is the number of clusters.

493 The main loops of GFA and EGFA in data clustering are the same as the description in Section 2.1
494 and Section 2.2.3.

495 **3.2.2 Datasets and performance evaluation**

496 The datasets listed in Table 5 are the well-known real datasets from the UCI Machine Learning
497 Repository [36], which are usually used to test the performance of clustering algorithms. These three real
498 datasets are chosen from a series of past research in clustering. Table 5 shows the number of instances,
499 the number of attributes, the number of clusters, and the distribution of the three datasets. Specifically,
500 The Iris dataset consists of 150 instances with 4 attributes. The Seeds dataset consists of 210 instances
501 with 7 attributes. The Wine dataset consists of 178 instances with 13 attributes. There are 3 clusters of the
502 three real datasets. This paper applies GFA and EGFA in clustering, and compared the results of them
503 with k-means.

504

505 Table 5.

506 The real datasets for testing GFA, EGFA and k-means

Datasets	Number of instances	Number of attributes	Number of clusters	distribution
Iris	150	4	3	50/50/50
Seeds	210	7	3	70/70/70
Wine	178	13	3	59/71/48

507

508 In order to compare the performance of GFA, EGFA and k-means, The Adjusted Rand index (ARI)
 509 is adopted to assess clustering results of the three algorithms. The adjusted Rand Index is usually used to
 510 measures the agreement between two partitions. It is the corrected-for-chance version of Rand index (RI),
 511 which is simply defined as $RI = \frac{a+b}{a+b+c+d}$ (The range of the Rand index is between 0 and 1. When
 512 the two partition agree perfectly, the Rand index is 1. More details about Rand index are presented in
 513 [37] [38]). The original Adjusted Rand index is defined as Eq. (16).

$$ARI = \frac{Index - ExpectedIndex}{MaxIndex - ExpectedIndex} = \frac{\sum_i \binom{n_{ij}}{2} - \left[\sum_i \binom{a_i}{2} \sum_j \binom{b_j}{2} \right] / \binom{n}{2}}{\frac{1}{2} \left[\sum_i \binom{a_i}{2} + \sum_j \binom{b_j}{2} \right] - \left[\sum_i \binom{a_i}{2} \sum_j \binom{b_j}{2} \right] / \binom{n}{2}}, \quad (16)$$

515 the bigger value the ARI is, the more agreement of the two partitions have. We adopt the Adjusted Rand
 516 index as the measure of the experimental results, and the Readers can refer [37] [38] for more details
 517 about how Adjusted Rand index assesses the agreement between two partitions.

518 3.2.3 Parameter settings

519 The settings of parameters for GFA, EGFA and k-means are showed in Table 6. The size of population is
 520 set as 20 for GFA and EGFA. The maximum number of iterations is set 100 for all three algorithms.
 521 There is a trick to setting the number of clusters in this research. Firstly, EGFA runs several times in
 522 different number of clusters. Then the value of ARI of those results is calculated. Lastly, the number of
 523 clusters is decided according the value of ARI, the one with largest value of ARI is desirable. Fig. 12
 524 shows the average value of ARI for 30 trials on seeds dataset in different number of clusters. As Fig.12
 525 shows the ARI is largest when the number of clusters is 3. In this way, the number of clusters is set 3 for

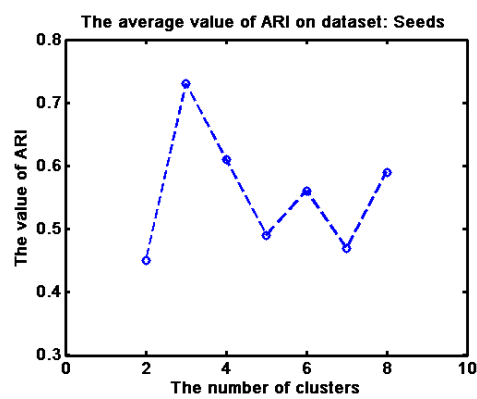
526 datasets: Iris, Seeds and Wine finally.

527 Table 6.

528 The parameters setting of GFA, EGFA and k-means

Parameters setting	Population Size	Max Number of iterations	Number of clusters
GFA	20	100	3
EGFA	20	100	3
k-means	-	100	3

529



530

531 Fig. 12 The average value of ARI on Seeds dataset in different number of clusters

532

533 3.2.4 Experimental results and analysis

534 The comparisons of three algorithms: GFA, EGFA and k-means for 30 trials on three real datasets in

535 average value of Adjusted Rand index (ARI) are shown in Table 7. Table 7 shows that the EGFA

536 outperforms GFA and k-means on the three real datasets: Iris, Seeds, and Wine. Specifically, EGFA has

537 the highest value of ARI among the three algorithms, which indicates that EGFA has the best performance

538 compared with the original GFA and k-means in the three real datasets. In addition, GFA performs better

539 than k-means on the datasets: Wine and Seeds, and k-means performs better than GFA on dataset Iris.

540

541

542

543

544 Table 7

545 The results of GFA, EGFA and k-means in ARI

ARI	GFA	EGFA	k-means
Iris	0.5791	0.6846	0.6836
Seeds	0.7027	0.7302	0.6998
Wine	0.3676	0.3715	0.3499

546 **4. Conclusions and Future work**

547 In this research, a novel EGFA is presented based on the original GFA. A novel accuracy improvement
548 strategy called Dust Sampling (DS) is employed to quickly find the so-called optimal space that contains
549 the optimal solution in search space. Another novel strategy named Explosion Operation is adopted to
550 decrease the probability of dust falling into local optima, and the formulae for iteration are modified. Six
551 benchmark problems and three real datasets previously used from literatures in unconstrained
552 optimization are chosen to evaluate the performance of EGFA. The experimental results demonstrate that
553 the proposed EGFA has achieved excellent performance in terms of efficiency, accuracy, and the
554 capability of solving real world problems. All the results indicate that EGFA is of well convergence and
555 higher search efficiency.

556 It is noted that the solutions EGFA finds are frequently closer to the actual optimal solutions than
557 the other three algorithms in the lower dimensions on all the six benchmark problems and three real
558 datasets, but at the same time, we also notice the fact that all the four optimization algorithms face
559 challenges when dealing with problems in higher dimensions in terms of in accuracy and running time,
560 especially when the dimension is larger than 20. This motivates us to make more efforts in our future
561 research to investigate how to further improve EGFA along this line. The study on complex unconstrained
562 optimization problems in higher dimensions by EGFA is in progress, and we will also further investigate
563 how to find more effective methods to adjust the parameters according to the characteristics of specific
564 problems.

565 **Acknowledgement**

566 This research was funded by the National Natural Science Foundation of China (Nos.61572227,
567 61772227, 61702214), the Development Project of Jilin Province of China (Nos 20170101006JC,

568 20180414012GH, 20170203002GX, 20190201293JC), Zhuhai Premier-Discipline Enhancement
569 Scheme (Grant 2015YXXK02) and Guangdong Premier Key-Discipline Enhancement Scheme (Grant
570 2016GDYSZDXK036). This work was also supported by Jilin Provincial Key Laboratory of Big Data
571 Intelligent Computing (No. 20180622002JC).

572 **References**

- 573 [1] B. Chatterjee, *Steepest Descent Method*: Springer US, 2013.
- 574 [2] F. Ahmad, E. Tohidi, and J. A. Carrasco, "A parameterized multi-step Newton method for solving
575 systems of nonlinear equations," *Numerical Algorithms*, vol. 71, pp. 1-23, 2016.
- 576 [3] J. Zhao, E. A. H. Vollebregt, and C. W. Oosterlee, "A fast nonlinear conjugate gradient based method
577 for 3D concentrated frictional contact problems," *Journal of Computational Physics*, vol. 288, pp.
578 86-100, 2015.
- 579 [4] R. H. Byrd, S. L. Hansen, J. Nocedal, and Y. Singer, "A Stochastic Quasi-Newton Method for Large-
580 Scale Optimization," *Siam Journal on Optimization*, vol. 26, 2015.
- 581 [5] M. A. Salido, J. Escamilla, A. Giret, and F. Barber, "A genetic algorithm for energy-efficiency in
582 job-shop scheduling," *The International Journal of Advanced Manufacturing Technology*, vol. 85,
583 pp. 1303-1314, 2016.
- 584 [6] E. Elyan and M. M. Gaber, "A Genetic Algorithm Approach to Optimising Random Forests Applied
585 to Class Engineered Data," *Information Sciences*, 2016.
- 586 [7] T. Liao, K. Socha, M. A. M. D. Oca, and T. Stützle, "Ant Colony Optimization for Mixed-Variable
587 Optimization Problems," *IEEE Transactions on Evolutionary Computation*, vol. 18, pp. 503-518,
588 2014.
- 589 [8] Z. Wang, H. Xing, T. Li, and Y. Yang, "A Modified Ant Colony Optimization Algorithm for Network
590 Coding Resource Minimization," *IEEE Transactions on Evolutionary Computation*, vol. 20, pp. 1-
591 1, 2015.
- 592 [9] J. Kennedy and R. Eberhart, *Particle swarm optimization*: Springer US, 2011.
- 593 [10] X. L. Wen, J. C. Huang, D. H. Sheng, and F. L. Wang, "Conicity and cylindricity error evaluation
594 using particle swarm optimization," *Precision Engineering*, vol. 34, pp. 338-344, 2010.
- 595 [11] J. Kennedy and R. Eberhart, "Particle swarm optimization," *IEEE International Conference on*

- 596 Neural Networks, vol. 4, pp. 1942-1948, 1995.
- 597 [12] B. Xing and W. J. Gao, *Innovative Computational Intelligence: A Rough Guide to 134 Clever*
598 *Algorithms*: Springer Publishing Company, Incorporated, 2013.
- 599 [13] D. Karaboga and B. Basturk, "A powerful and efficient algorithm for numerical function
600 optimization: artificial bee colony (ABC) algorithm," *Journal of Global Optimization*, vol. 39, pp.
601 459-471, 2007.
- 602 [14] C. J. A. B. Filho, F. B. D. L. Neto, A. J. C. C. Lins, A. I. S. Nascimento, and M. P. Lima, *Fish School*
603 *Search*: Springer Berlin Heidelberg, 2009.
- 604 [15] K. M. Passino, *Bacterial Foraging Optimization*: IGI Global, 2010.
- 605 [16] S. C. Chu and P. W. Tsai, "Computational intelligence based on the behavior of cats," *International*
606 *Journal of Innovative Computing Information & Control Ijicic*, vol. 3, pp. 163-173, 2006.
- 607 [17] O. K. Erol and I. Eksin, *A new optimization method: Big Bang-Big Crunch*: Elsevier Science Ltd.,
608 2006.
- 609 [18] R. A. Formato, "Central Force Optimization: a New Metaheuristic with Applications in Applied
610 Electromagnetics," vol. 77, pp. 425-491, 2007.
- 611 [19] E. Rashedi, H. Nezamabadi-Pour, and S. Saryazdi, "GSA: A Gravitational Search Algorithm,"
612 *Intelligent Information Management*, vol. 4, pp. 390-395, 2012.
- 613 [20] A. Y. S. Lam and V. O. K. Li, "Chemical-Reaction-Inspired Metaheuristic for Optimization," *IEEE*
614 *Transactions on Evolutionary Computation*, vol. 14, pp. 381-399, 2010.
- 615 [21] S. A. Salem, "BOA: A novel optimization algorithm," in *International Conference on Engineering*
616 *and Technology*, pp. 1-5, 2012.
- 617 [22] M. Zheng, G. Liu, C. Zhou, Y. Liang, and Y. Wang, "Gravitation field algorithm and its application
618 in gene cluster," *Algorithms for Molecular Biology*, vol. 5, pp. 1-11, 2010.
- 619 [23] M. Zheng, Y. Sun, G. Liu, Y. Zhou, and C. Zhou, "Improved Gravitation Field Algorithm and Its
620 Application in Hierarchical Clustering," *PloS One*, vol. 7, p. e49039, 2012.
- 621 [24] M. Zheng, G. X. Liu, Y. Zhou, and C. G. Zhou, "Reconstruction of gene regulatory network based
622 on gravitation field algorithm," *Journal of Jilin University*, vol. 44, pp. 427-432, 2014.
- 623 [25] V. S. Safronov, "Evolution of the protoplanetary cloud and formation of the earthand planets," *Trans.*
624 *NASA TT F-677*, 1972.
- 625 [26] L. Huang, X. Hu, Y. Wang, F. Zhang, Z. Liu, and W. Pang, "Gravitation field algorithm with optimal

- 626 detection for unconstrained optimization," in International Conference on Systems and Informatics,
627 2017, pp. 1411-1416.
- 628 [27] G. P. Zhu and S. Kwong, "Gbest-guided artificial bee colony algorithm for numerical function
629 optimization," *Applied Mathematics and Computation*, vol. 217, pp. 3166-3173, Dec 1 2010.
- 630 [28] D. E. Goldberg. "Genetic Algorithms in Search, Optimization and Machine Learning ", Addison-
631 Wesley Pub. Co. pp. 2104–2116, 1989.
- 632 [29] G. Steenackers and P. Guillaume, "Bias-specified robust design optimization: A generalized mean
633 squared error approach," *Computers & Industrial Engineering*, vol. 54, pp. 259-268, 2008.
- 634 [30] A. Majumder, "Application of Standard Deviation Method Integrated PSO Approach in
635 Optimization of Manufacturing Process Parameters," *Handbook of Research on Artificial
636 Intelligence Techniques & Algorithms*, 2015.
- 637 [31] W. Pang and G. M. Coghill, "QML-AiNet: An immune network approach to learning qualitative
638 differential equation models," *Applied Soft Computing*, vol. 27, pp. 148-157, 2015.
- 639 [32] S. Siegel and N. J. J. Castellan, "Non-Parametric Statistics for Behavioral Sciences," *American
640 Catholic Sociological Review*, vol. 18, 1957.
- 641 [33] G. W. Corder and D. I. Foreman, *Nonparametric Statistics for Non-Statisticians: A Step-by-Step
642 Approach*, 2009.
- 643 [34] S. García, D. Molina, M. Lozano, and F. Herrera, "A study on the use of non-parametric tests for
644 analyzing the evolutionary algorithms' behavior: a case study on the CEC'2005 Special Session on
645 Real Parameter Optimization," *Journal of Heuristics*, vol. 15, pp. 617-644, 2009.
- 646 [35] R. Duwairi and M. Abu-Rahmeh, "A novel approach for initializing the spherical K-means clustering
647 algorithm," *Simulation Modelling Practice and Theory*, vol. 54, pp. 49-63, May 2015.
- 648 [36] D. Dua and C. Graff, "UCI Machine Learning Repository [<http://archive.ics.uci.edu/ml>]. " Irvine,
649 CA: University of California, School of Information and Computer Science, 2019.
- 650 [37] D. Steinley, M. J. Brusco, and L. Hubert, "The Variance of the Adjusted Rand Index," *Psychological
651 Methods*, vol. 21, pp. 261-272, Jun 2016.
- 652 [38] R. Brouwer, "Extending the rand, adjusted rand and jaccard indices to fuzzy partitions," *Journal of
653 Intelligent Information Systems*, vol. 32, pp. 213-235, Jun 2009.